

# Staircase approximation validity for arbitrary-shaped gratings

Evgeny Popov, Michel Nevière, Boris Gralak, and Gérard Tayeb

*Institut Fresnel, Unité Mixte de Recherche du Centre National de la Recherche Scientifique 6133, Faculté des Sciences et Techniques de St-Jérôme, 13397 Marseille Cedex 20, France*

Received March 23, 2001; revised manuscript received May 31, 2001; accepted May 31, 2001

An electromagnetic study of the staircase approximation of arbitrary shaped gratings is conducted with three different grating theories. Numerical results on a deep aluminum sinusoidal grating show that the staircase approximation introduces sharp maxima in the local field map close to the edges of the profile. These maxima are especially pronounced in TM polarization and do not exist with the original sinusoidal profile. Their existence is not an algorithmic artifact, since they are found with different grating theories and numerical implementations. Since the number of the maxima increases with the number of the slices, a greater number of Fourier components is required to correctly represent the electromagnetic field, and thus a worsening of the convergence rate is observed. The study of the local field map provides an understanding of why methods that do not use the staircase approximation (e.g., the differential theory) converge faster than methods that use it. As a consequence, a 1% accuracy in the efficiencies of a deep sinusoidal metallic grating is obtained 30 times faster when the differential theory is used in comparison with the use of the rigorous coupled-wave theory. A theoretical analysis is proposed in the limit when the number of slices tends to infinity, which shows that even in that case the staircase approximation is not well suited to describe the real profile. © 2002 Optical Society of America

OCIS codes: 050.1950, 050.1960, 260.2110, 000.4430.

## 1. INTRODUCTION

When almost 25 years ago Moharam and Gaylord published their first work<sup>1</sup> on a method for modeling diffraction gratings, a method later called the “rigorous coupled-wave (RCW) method,” they could probably hardly imagine how long would be the history of this method. A year later<sup>2</sup> they proposed to use the method for surface relief gratings. Although the method was initially designated for lamellar gratings, the idea that each grating profile could be represented as a staircase approximation of several or more layers of lamellar gratings naturally came to mind to extend the universality of the method. However, as happened sooner or later with all the methods, problems arose in dealing with deeper gratings. The first reason was that the growing exponential terms<sup>3,4</sup> eliminated using an approach derived from chemistry<sup>5,6</sup> known as the *R*-matrix propagation algorithm, which was soon replaced by the much simpler *S*-matrix propagation algorithm.<sup>7,8</sup> This, however, did not help when highly conducting gratings were used in TM polarization, with the magnetic-field vector parallel to the grooves. Recently Lalanne *et al.*<sup>9</sup> found an empirical solution for this problem, which was put on a strong mathematical basis by Li.<sup>10</sup> The rules pointed out by Li were used by Popov and Nevière<sup>11,12</sup> to propose a fast converging formulation of the differential theory for arbitrary-shaped gratings, which gave spectacular results in TM polarization.

The current situation is that the RCW theory is very suitable for lamellar metallic and dielectric gratings because it gives rapidly converging results. The question that remains is whether the method can have the same success when applied to arbitrary profiles. Despite the

long history of its development, there are only a few numerical results published in the literature that address the question. Moreover, these studies concern either dielectric gratings or metallic gratings in TE polarization only. The few published studies on deep metallic gratings with profile different from the lamellar one<sup>13</sup> do not present sufficient accuracy, because the staircase approximation only contains only a few “levels” (or “slices”).<sup>14</sup>

The aim of this paper is to present a comparative study of three different methods based on the differential theory. These are the classical differential method, recently improved by using the fast Fourier factorization (FFF) technique,<sup>11,12</sup> the RCW method, and the modal method.<sup>15–18</sup> The choice is linked to the fact that the three methods are similar: The solution of Maxwell differential equations is sought by projecting the solution on some basis of functions of *x* (see Fig. 1), which are periodic along the grating surface. Then the field dependence in the vertical (*y*) direction along the groove height is found by using different techniques:

1. The classical differential method uses Fourier basis in *x* with numerical integration of a finite set of ordinary differential equations in *y*.
2. The RCW method also uses Fourier basis in *x*, but the grating is lamellar. Thus the coefficients of the differential system are constant along *y*, and the method avoids numerical integration by using an eigenvalue/eigenvector technique to find the solution of the set of differential equations.
3. The modal method projects the field components on a basis of functions of *x*, which are rigorous solutions of the Maxwell equations, and boundary conditions along *x*

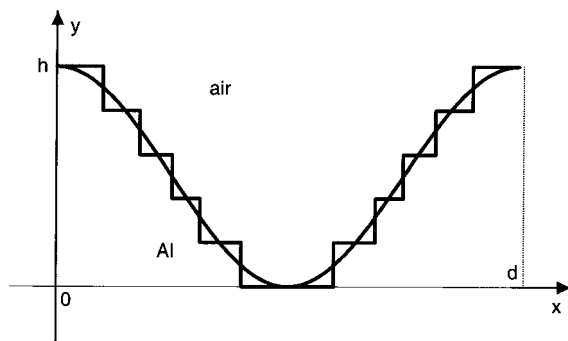


Fig. 1. Schematic representation of a sinusoidal profile and a five-stair approximation of the same profile, together with some notations used in the text.

(modes), assuming infinite height of the grooves along  $y$ . The solution of the diffraction problem is found in this basis by matching a superposition of the modes (with unknown coefficients) with the Rayleigh expansion in the substrate and the cladding.

It is clear that the RCW and the modal method are well adapted to lamellar gratings, while the classical differential method can be used for arbitrary profiles but pays a price by using numerical integration. In general, the modal method requires fewer numbers of basis functions than the methods based on the Fourier representation. On the other hand, finding the modes is more difficult for metallic gratings, but the problem is already solved.<sup>15–18</sup>

It is important to note that, when applied to a given grating, consisting of a smooth profile represented with a fixed number of slices in the staircase approximation, the differential and the RCW methods give identical results, even when the number of the Fourier components is not sufficient to correctly represent the field. This fact shows that if a problem exists, it is not due to the techniques used to integrate the set of equations, i.e., it is not an algorithmic artifact. However, the results obtained for the discretized (staircaselike) and nondiscretized profile may differ significantly. The aim of this paper is to study this problem.

## 2. SINUSOIDAL ALUMINUM GRATING IN TE POLARIZATION

We begin by studying the staircase approximation in TE polarization (electric field vector parallel to the grooves). The grating under investigation is made of aluminum and has a sinusoidal profile with period  $d = 0.5 \mu\text{m}$  and groove depth  $h = 0.2 \mu\text{m}$ . This is a typical widely used grating in lasers and spectroscopy, because it is characterized by almost perfect blazing (very-high diffraction efficiency) in TM polarization in a wide spectral range in the visible.

The grating is illuminated at an angle  $\theta_i = 40^\circ$  with light of a wavelength  $\lambda = 0.6328 \mu\text{m}$ ; thus two diffracted orders propagate in air. The aluminum complex refractive index is  $n_{Al} = 1.3 + i7.6$ . In what follows we are interested mainly in the convergence rate of the different methods as a function of the so-called truncation parameter  $N$ , which characterizes the number of Fourier components (or modes) used in the field expansion along  $x$ , this

number being equal to  $2N + 1$  (varying from  $-N$  to  $N$  in the case of Fourier basis). However, to start with, it is interesting to know the number  $M$  of slices that are necessary to correctly represent the sinusoidal profile (Fig. 1). As a rule of thumb, one can expect that the characteristic dimensions of the stairs must be less than  $\lambda/50$ . And, indeed, Fig. 2 points out that a sufficient accuracy ( $>1\%$ ) is already obtained with approximately 15 slices. The figure represents the mean error, equal to the sum of the relative errors in all the propagating orders, divided by their number. In the calculations, the truncation parameter  $N$  is fixed equal to 90, a value sufficient to provide convergent results for both the differential and the RCW method when they are applied to the same discretized profile. The error decreases monotonically and becomes close to  $10^{-4}$  for  $M > 200$ . The reference values to calculate the error are calculated by two independent methods, namely, the integral method<sup>19</sup> and the method of fictitious sources.<sup>20</sup>

The convergence with respect to the truncation parameter  $N$  for the three methods is presented in Fig. 3. The differential method is applied to the smooth sinusoidal

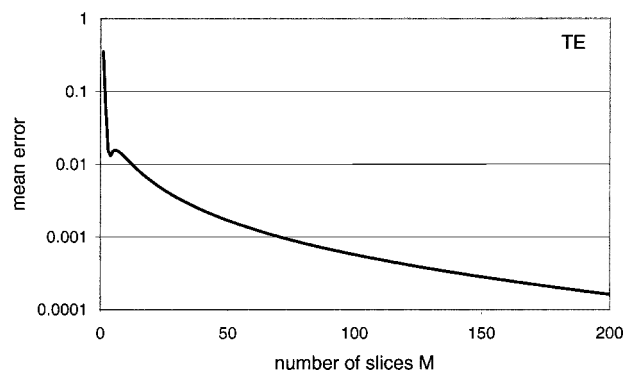


Fig. 2. Mean error in the reflected diffraction orders as a function of the number of slices in the staircase approximation (Fig. 1) of an aluminum grating with a sinusoidal groove profile, period  $d = 0.5 \mu\text{m}$ , groove depth  $h = 0.2 \mu\text{m}$ , aluminum refractive index  $n_{Al} = 1.3 + i7.6$ , illuminated at  $40^\circ$  incidence with TE polarized light with wavelength  $\lambda = 0.6328 \mu\text{m}$ .

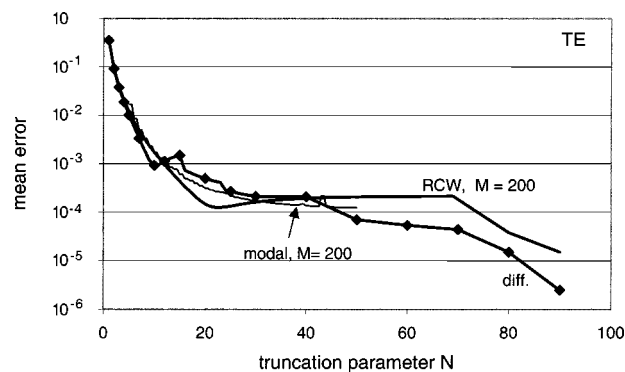


Fig. 3. Convergence of the mean error for the grating with parameters given in Fig. 2 as a function of the truncation parameter  $N$ , the number of the Fourier components or modes being equal to  $2N + 1$ . The RCW method (heavy solid curve) and the modal method (thin curve) are used with  $M = 200$  slices, the differential method (curve "diff.") is applied to the smooth sinusoidal profile. TE polarization.

profile, and the modal and the RCW methods are applied to the staircase profile with  $M = 200$  slices. The results of the modal method are not presented for large  $N$ , because the corresponding computer code deals with the more general case of crossed gratings in conical diffraction, which needs more computational resources for the same values of  $N$ .

For this polarization we can conclude that the three methods lead to the same error for a given truncation and that a relative error of less than 0.1% is obtained with  $N = 10$ , which is a good indication for short computation times.

### 3. TM CONVERGENCE

In TM polarization, the zeroth-order efficiency is very close to zero, so that the relative error is an unreliable characteristic, and thus in what follows we present the convergence rates of the  $-1$ st order efficiency. Figure 4 presents the calculated efficiency as a function of  $N$  for the different methods and the different numbers of slices  $M$ . Again, the differential method is applied to the real smooth sinusoidal profile. Its numerical implementation is described in Refs. 11 and 12; i.e., a set of first-order differential equations is integrated taking as unknown functions the Fourier components of both electric and magnetic fields; the FFF is used to ameliorate the convergence. Again we find that when applied to the staircase profile, the differential method gives the same results as the RCW method. This proves that the results do not depend on the algorithm used for the integration: when implementing the differential method, we independently applied the Runge–Kutta and Adams–Moulton techniques; in addition, two codes developed independently by two authors have been used to confirm the results.

For the smooth profile (curve “diff.” in Fig. 4), the asymptotic value approaches 1% as soon as  $N = 11$  (23 Fourier components). Using thirteen layers in the  $S$ -matrix propagation algorithm and four steps of integration per layer, the calculation time is 1 s on a PC Pentium III (800 MHz).

When  $M = 1$ , the sinusoidal grating is replaced by a lamellar one; Fig. 4(a) shows that the RCW and the modal method give results having the same convergence rate as a function of  $N$ . The convergence rate for the discretized profile is the same as for the smooth sinusoidal profile (curve “diff.”), although the asymptotic efficiency differs significantly for the two profiles, which is not surprising. This shows that the single-step approximation is rather poor and that the number of slices  $M$  must be increased. When  $M$  is increased to  $\sim 20$  [Fig. 4(b)], the asymptotic value of the efficiency approaches to within 1% of the efficiency of the smooth profile (almost in the same way as in the TE polarization, where  $M = 15$  was sufficient). However, the number of Fourier coefficients (or modes, for the modal method) required to approach the asymptotic value increases for both the RCW and the modal methods. To obtain the same accuracy (error  $< 1\%$ ), it is necessary to increase  $N$  up to 20 for the modal method and up to 50 for the RCW method (i.e., 101 Fourier spatial harmonics), requiring 30 s calculation time, which has to be com-

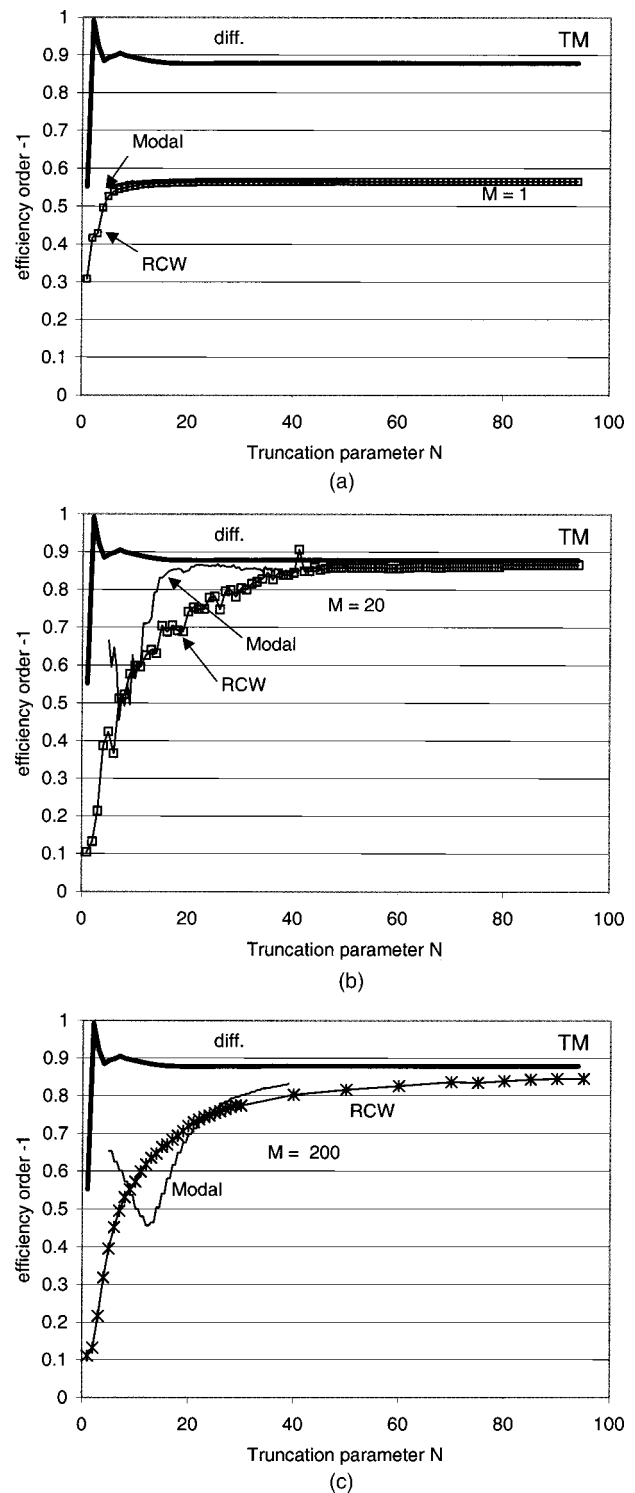


Fig. 4. Convergence of the  $-1$ st order efficiency in TM polarization of the RCW and modal methods (indicated in the figure) (a) for a single-step ( $M = 1$ ) lamellar grating, (b) for a staircase grating with  $M = 20$ , (c)  $M = 200$ , compared with the convergence of the differential method for a smooth sinusoidal profile (curve “diff.”). The grating parameters are given in Fig. 2.

pared with 1 s necessary for the differential method when modeling the smooth sinusoidal profile with the same accuracy.

The situation becomes worse for  $M = 200$ , Fig. 4(c). Even  $N = 100$  is not sufficient for the RCW method to

converge (we stress again that the same results are obtained when the differential method is applied to the staircase profile). To explain this surprising deterioration of the convergence rate, it is necessary to study the field map inside the grooves.

#### 4. NEAR-FIELD MAPS: TM POLARIZATION

In order to understand the poor convergence of all the methods for staircase profiles in TM polarization, we analyzed the near-field maps for two discretized profiles, with five and twenty slices, as well as the field map of the smooth sinusoidal profile. In TM polarization the magnetic-field vector is parallel to the grooves (i.e., to the  $z$  axis) and is a continuous function even across the grating surface. The electric field has  $x$  and  $y$  components,  $E_x$  and  $E_y$ , respectively. For five slices, Fig. 5 shows the surface of  $|E_x|^2$  as a function of  $x$  and  $y$  inside the groove, characterized by a smoothly varying background with sharp peaks close to the profile ridges. The field maps for a staircase profile were obtained with the RCW method, while the differential method was used for the sinusoidal profile (see Fig. 8 below). For a better analysis, Figs. 6(a) and 6(b) represent gray-scale maps of the two components  $|E_x|^2$  and  $|E_y|^2$ , respectively. Strong maxima near the step ridges are observed, which could be expected for a metallic grating having sharp ridges, owing to the charge accumulation at the ridges. However, the maxima of  $|E_x|^2$  and  $|E_y|^2$  do not occur at the same location. This is due to the fact that the two components of the electric-field vector are discontinuous across the different segments of the profile:  $|E_x|^2$  is continuous across the horizontal part (parallel to the  $x$  axis). Its jump across the vertical segments (which are due to the large jump of the refractive index) allows for the existence of the sharp peaks on the vertical segments, while the continuity

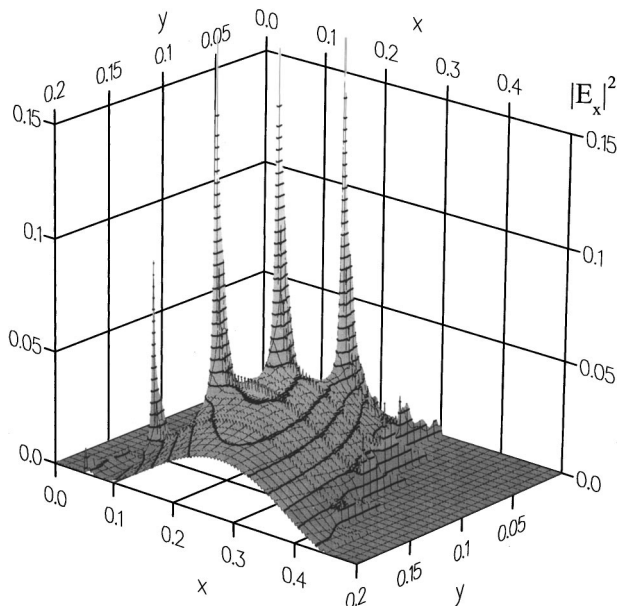


Fig. 5. Three-dimensional view of the distribution of the  $x$  component of the field squared inside the groove for a five-step staircase approximation in TM polarization.

along the  $y$  axis and the fact that the electric field is weak inside the metal limits  $|E_x|^2$  in the vicinity of the horizontal segments. The opposite is true for  $|E_y|^2$ , which explains why its maxima occur on the horizontal segments. In any case, the maxima of the two components occur close to the ridge, as already discussed.

It must be stressed that the existence of these sharp peaks is not due to Gibbs phenomena arising from the representation of the discontinuous functions  $E_x$  and  $E_y$  by truncated Fourier series. The convergence of the field maps was checked and no visible difference was found when going from 161 to 321 Fourier components.

A greater number of stairs introduces a larger number of edges and smaller features of the profile segments. A three-dimensional view of  $|E_x|^2$  and  $|E_y|^2$  as a function of  $x$  and  $y$  for  $M = 20$  is shown in Fig. 7 with a zoom inside the groove region where the field is stronger. Well-pronounced peaks of  $|E_x|^2$  and  $|E_y|^2$  are observed close to the edges in the same manner as for  $M = 5$ , and again the peaks of  $|E_x|^2$  and  $|E_y|^2$  are spatially separated. The shorter length of the profile segments leads to narrower peaks.

The fact that close to the ridges of the staircase profile one observes regions with field enhancement explains the deterioration of the convergence rate of the methods with increasing number of slices: The greater the number of stairs, the closer and thinner the maxima and the greater their number and thus the greater the number of Fourier components required to correctly represent the field in the form of truncated series. In the modal method, this leads to the increase in the number of modes inside the grooves, although not to as great an extent as for the RCW method, probably because the modes are not equidistant spectrally, as the Fourier harmonics are.

The field enhancement close to the ridges occurs when any of the three methods are used, and it is a real physical effect because the smooth profile is replaced with a staircaselike profile having ridges. To observe the difference, it is sufficient to compare the previous figures with the field map of the sinusoidal (nondiscretized) grating, presented in Fig. 8(a), obtained by use of the differential theory. A closer view [Fig. 8(b)] of the same region as was presented in Fig. 7(a) shows no peaks close to the profile, and the field inside the groove [on the left part of Fig. 8(b)] is the same as the background field (outside the peak region) inside the grooves in Fig. 7(a) (approximately equal to 0.30). The weak variations of the field in Fig. 8 come from the Gibbs phenomena, as the calculations were made using 201 Fourier components. The absence of sharp and narrow peaks of the field for the smooth profile explains the fast convergence of the differential method with respect to the number of Fourier components. As discussed in Section 3, 23 Fourier components are sufficient.

#### 5. NEAR-FIELD MAP: TE POLARIZATION

It is now necessary to explain the fast convergence of the three methods in TE polarization that are independent of the number of slices used in the staircase approximation. For that reason, it is worth studying the field maps. Only the region of the groove where the field is the strongest will be shown.

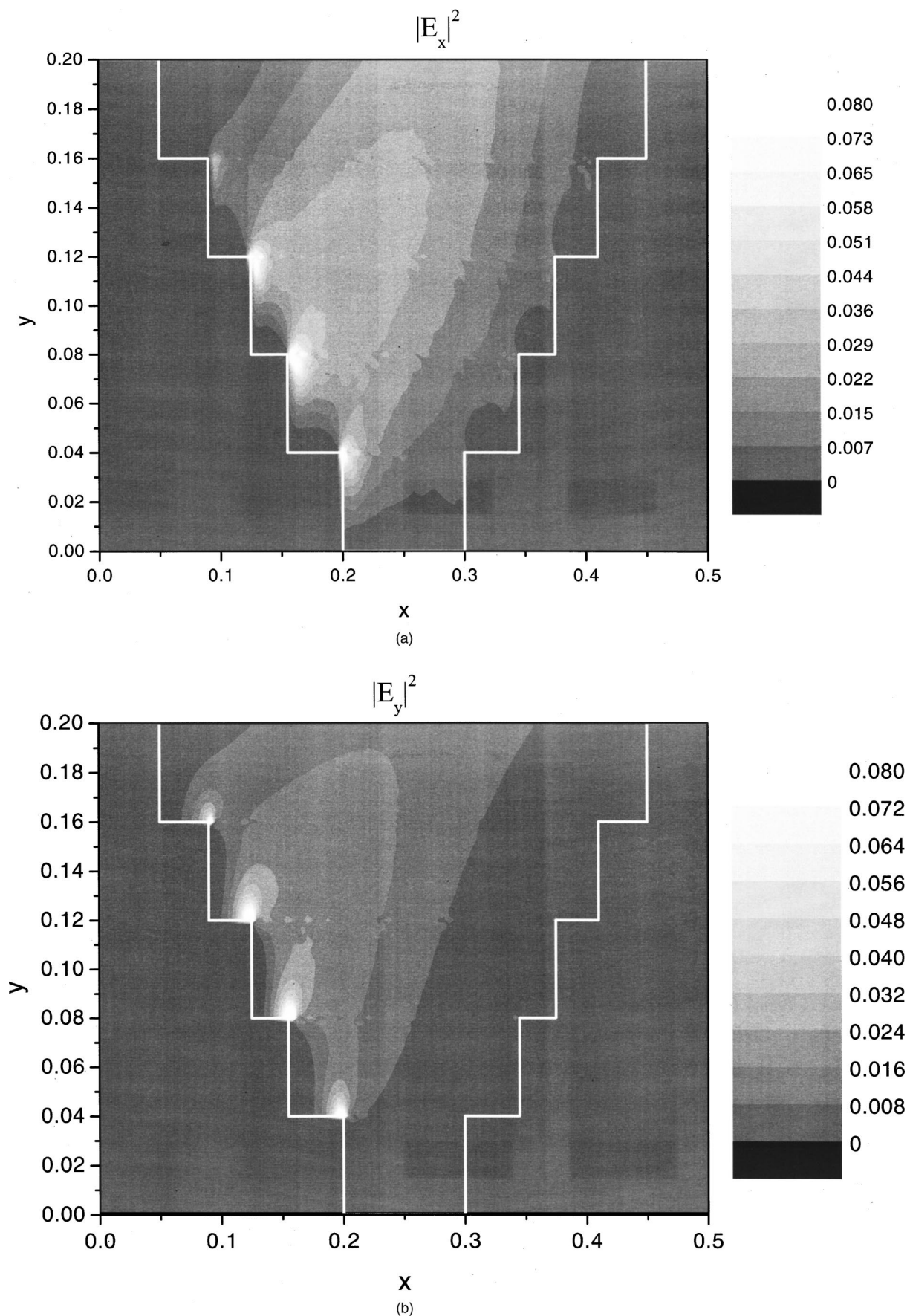
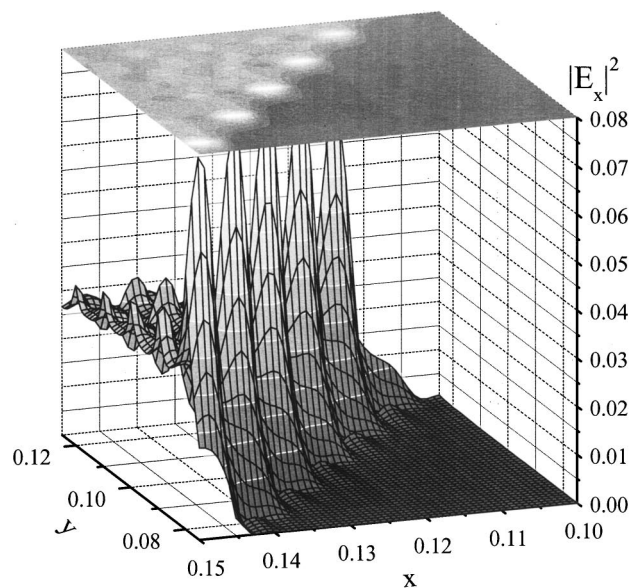
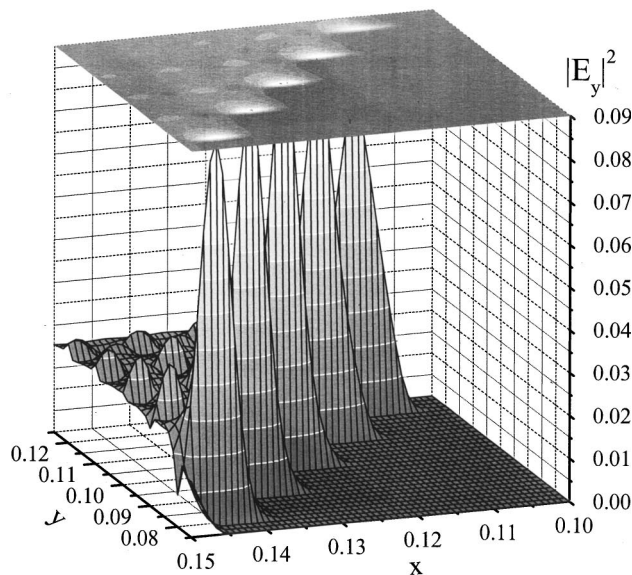


Fig. 6. Field map inside the groove of a five-step staircase grating in TM polarization. (a)  $|E_x|^2$ , (b)  $|E_y|^2$ .

In TE polarization, both electric and magnetic fields are continuous across the grating surface, because we consider nonmagnetic media. For  $M = 5$ , Figs. 9(a) and 9(b) show, respectively, the field maps of  $|H_x|^2$  and  $|H_y|^2$  for the same grating, studied in the previous sections, but in TE polarization. Peaks are found in the maps, but they rise to a lesser height from the smooth background than in the TM case. This is because the two components of the magnetic field (as well as the only component, the transverse one, of the electric field) are continuous functions when crossing the profile. As can be observed, the field “enters” the metal inside the stairs, and its variations are not so rapid as in the TM case. This fact

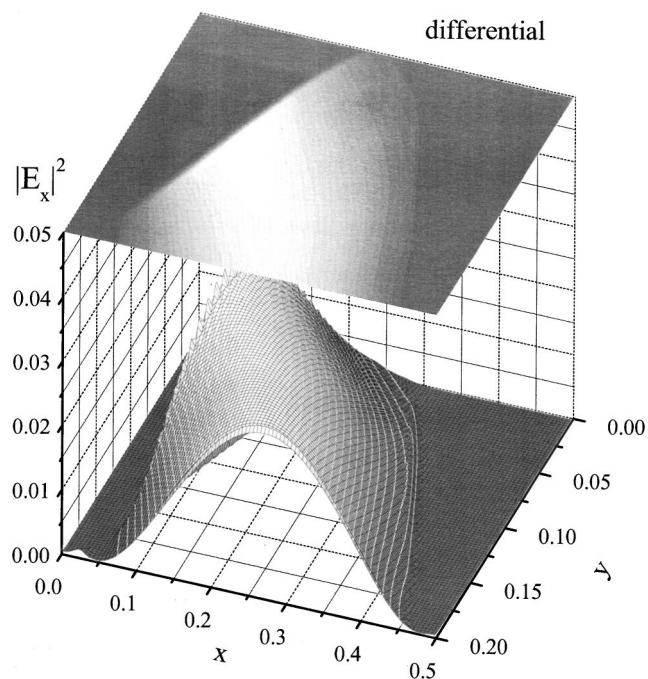


(a)

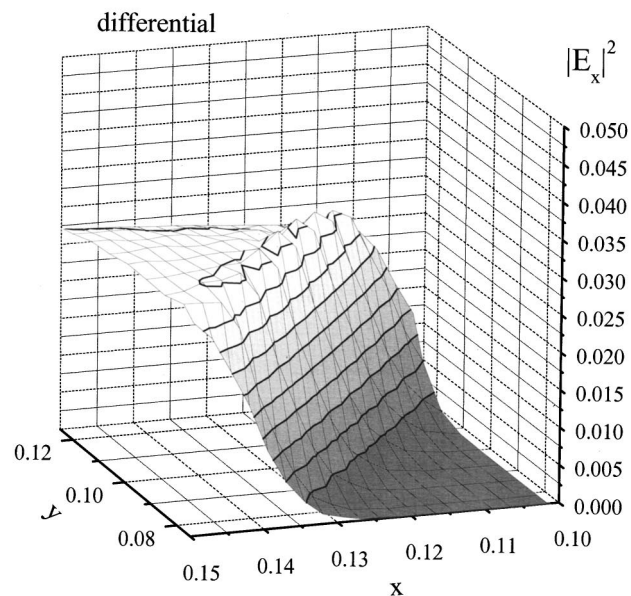


(b)

Fig. 7. Spatial field distribution in the vicinity of several steps inside the groove of a 20-step staircase profile, used to approximate the sinusoidal grating under study. TM polarization, (a)  $|E_x|^2$ , (b)  $|E_y|^2$ .



(a)



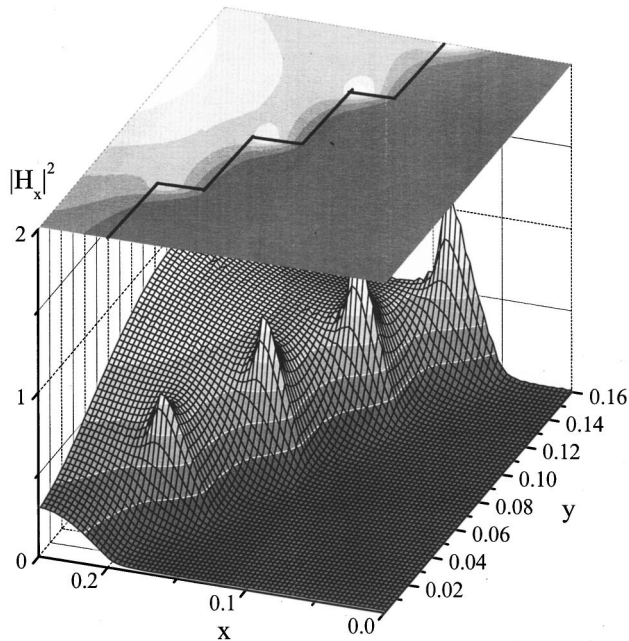
(b)

Fig. 8. Spatial distribution of  $|E_x|^2$  calculated for a nondiscretized sinusoidal profile in TM polarization. (a) The entire groove region as in Fig. 5, (b) the same region as presented in Fig. 7.

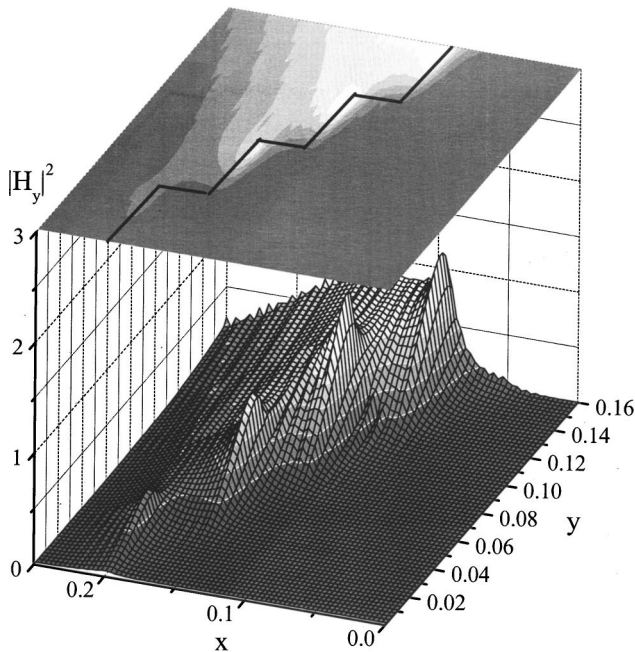
permits averaging the peaks when the number of slices is increased so that the step dimensions decrease. The effect could be observed for the 20-stairs approximation, as shown in Fig. 10, where the height of the peaks is further reduced, compared with five slices. Thus when  $M$  is increased in the TE case, it is not necessary to increase the number of Fourier harmonics in the field representation, which explains the better convergence rate, already observed in Fig. 3.

### 6. LIMIT FOR AN INFINITE NUMBER OF STAIRS

The effect of field “homogenization,” i.e., the averaging of the peaks when the number of slices is increased in the TE case (as shown in Figs. 9 and 10), raises the question of the possibility of such a homogenization in TM polarization, when the number of slices becomes so large that the adjacent maxima on the consecutive ridges start to overlap. Unfortunately, numerical requirements put a



(a)



(b)

Fig. 9. Spatial field distribution inside the groove region of a five-step staircase grating, presented in Fig. 1, in TE polarization. (a)  $|H_x|^2$ , (b)  $|H_y|^2$ .

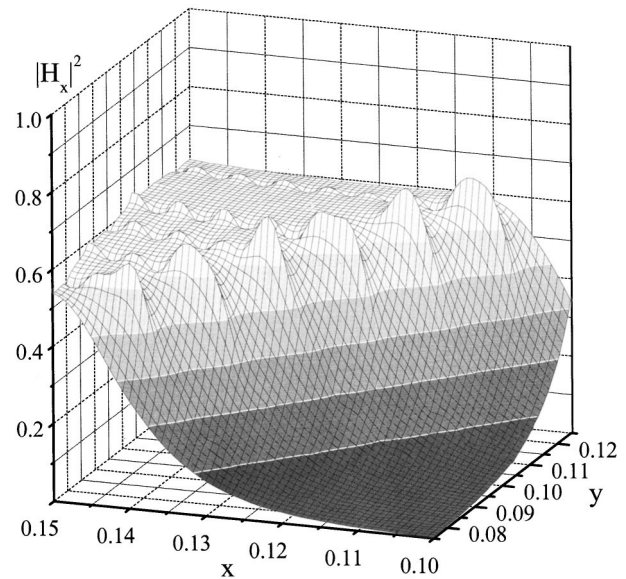


Fig. 10. Distribution of  $|H_x|^2$  inside the groove for a 20-step staircase approximation of the sinusoidal grating in TE polarization. Same groove region as in Fig. 7(a).

limit on the numerical investigations, so that no analysis of the near-field map for, say,  $M = 200$  or  $1000$  is possible, because this would require at least ten times more Fourier components to distinguish between Gibbs phenomena and the real-field fluctuations close to the ridges.

In any case, Fig. 4(c) already gives an answer about the effect when going to  $M = 200$ ; the convergence is poor. Some unreported results have been obtained for  $M = 500$ ; the convergence rate is not better. This means that no homogenization appears in the TM case, whatever the number of slices may be. In order to model this phenomenon, instead of increasing  $M$  (and thus  $N$ ), we may choose an alternative approach that consists of keeping  $M$  and  $N$  unchanged but increasing the wavelength. In fact, increasing the wavelength while preserving the number of slices (and thus their dimensions) is equivalent in the homogenization study to reducing the slice thickness and keeping the wavelength unchanged. The field maps inside the same groove region as shown in Fig. 7 are represented in Fig. 11 when the wavelength  $\lambda$  is increased 20 times, so that the dimensions of each step in the staircase profile with  $M = 20$  are of the order of  $\lambda/1300$ . As observed, no homogenization occurs, and sharp peaks are still present close to the step ridges. It is important to note that the three numerical methods use the same equations [see Eqs. (5)–(6) below] and the same boundary conditions along the vertical and the horizontal segments of the steps. Thus the physically strange result that no homogenization of the near field occurs may be linked to that fact; i.e., it may be a numerical artifact. The next part of this section deals with this problem.

In order to clarify whether these sharp peaks exist in the limit when  $M \rightarrow \infty$  and why they continue to play an important role in the far-field (efficiency) properties, although their width decreases with increasing the number of slices  $M$ , it is necessary to consider the limits of the Maxwell equations and of the boundary conditions for the electromagnetic field.

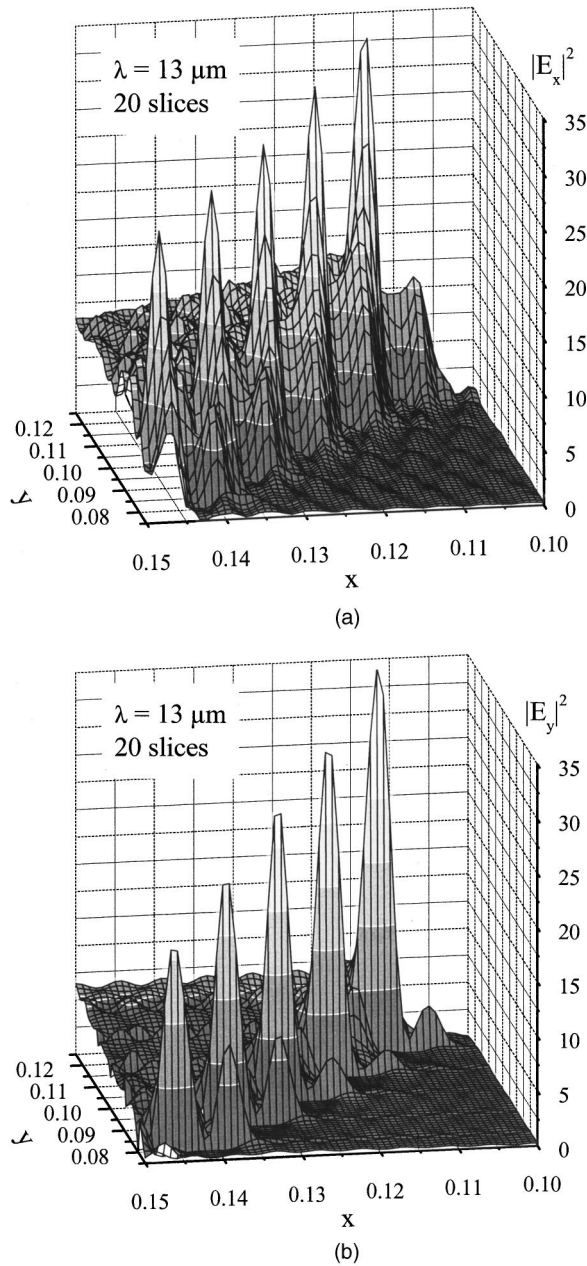


Fig. 11. Same as in Fig. 7, except for the wavelength  $\lambda = 13 \mu\text{m}$ .

Recent studies,<sup>10–12</sup> already mentioned in the introduction, have shown that correctly writing the Maxwell equations in the *infinite* Fourier basis does not guarantee that correct and stable numerical results will be obtained after truncation. The properties of truncated Fourier series of discontinuous functions require that the projection of the Maxwell equations on a *truncated* Fourier basis must depend on the direction of the vector normal to the grating surface, where the field and permittivity are discontinuous. Thus different forms of the equations have to be integrated for the smooth sinusoidal profile and for the staircaselike profile, whatever the number  $M$  of the stairs may be, including the case  $M \rightarrow \infty$ .

Without going into details, which can be found elsewhere,<sup>21</sup> the equations in the truncated Fourier space in TM polarization are

$$\frac{d[H_z]}{dy} = -i\omega \left\{ \left( \|\epsilon\| \|N_y^2\| + \left\| \frac{1}{\epsilon} \right\|^{-1} \|N_x^2\| \right) [E_x] - \left( \|\epsilon\| - \left\| \frac{1}{\epsilon} \right\|^{-1} \right) \|N_x N_y\| [E_y] \right\}, \quad (1)$$

$$\frac{d[E_x]}{dy} = -i\omega\mu_0[H_z] + i\alpha[E_y], \quad (2)$$

in which  $[E_y]$  is derived from

$$[E_y] = \left\{ \|\epsilon\| \|N_x^2\| + \left\| \frac{1}{\epsilon} \right\|^{-1} \|N_y\|^2 \right\}^{-1} \left\{ \frac{\alpha}{\omega} [H_z] + \left( \|\epsilon\| - \left\| \frac{1}{\epsilon} \right\|^{-1} \right) \|N_x N_y\| [E_x] \right\}. \quad (3)$$

$N_x$  and  $N_y$  are the components of the unit vector locally normal to the profile, square brackets denote a column vector symmetrically filled with Fourier components, double-straight-line brackets denote the truncated Toeplitz matrix composed of the Fourier components of the corresponding quantity:

$$\|f\|_{mn} = [f]_{m-n}. \quad (4)$$

$\epsilon$  is the permittivity, which depends on  $x$  and  $y$ ,  $\mu_0$  is the vacuum magnetic permeability,  $\omega$  is the circular frequency, and  $\alpha$  is a diagonal matrix with elements equal to  $\alpha_{mn} = (2\pi/\lambda)\delta_{mn}[\sin\theta_i + m(\lambda/d)]$ . Although the components of the normal vector are defined on the profile only, it is necessary to continue them everywhere in space in an appropriate way,<sup>11,12</sup> in order to obtain their Fourier coefficients.

The lamellar profile (or any of the vertical segments of the staircases profile) is characterized by  $N_x = 1$  and  $N_y = 0$ . Then Eqs. (1)–(3) are reduced to

$$\frac{d[H_z]}{dy} = -i\omega \left\| \frac{1}{\epsilon} \right\|^{-1} [E_x], \quad (5)$$

$$\frac{d[E_x]}{dy} = -i\omega\mu_0[H_z] + i\alpha \|\epsilon\|^{-1} \frac{\alpha}{\omega} [H_z]. \quad (6)$$

The classical differential method without the FFF improvement uses a similar set of equations derived from Eqs. (1)–(3) with  $N_x = 0$  and  $N_y = 1$ :

$$\frac{d[H_z]}{dy} = -i\omega \|\epsilon\| [E_x], \quad (7)$$

$$\frac{d[E_x]}{dy} = -i\omega\mu_0[H_z] + i\alpha \left\| \frac{1}{\epsilon} \right\| \frac{\alpha}{\omega} [H_z]. \quad (8)$$

Without truncation, i.e., when an infinite number of Fourier components is considered,  $\|\epsilon\| = \|1/\epsilon\|^{-1}$  and the three formulations are equivalent. However, this is not possible numerically, and they give quite different results for a finite  $N$ .

It is important to note that whatever the value of  $M$ , in the case of the staircase profile both the differential and the RCW method use Eqs. (5) and (6), whereas for the smooth profile one has to use the system of Eqs. (1)–(3). This means that in the limit of  $M \rightarrow \infty$ , the sets of equa-

tions to integrate are different if  $N$  is finite. It is thus inappropriate to expect identical results for the smooth and the staircase profiles. Moreover, if we now consider the different field components on the grating profile, whatever the value of  $M$  is,  $E_x$  is continuous across the horizontal segments (where  $E_y$  is discontinuous) and discontinuous along the vertical parts (where  $E_y$  is continuous). None of the two situations is valid for a continuous sinusoidal profile, for which the continuous (tangential) and discontinuous (normal) components are neither horizontal nor vertical (except at the bottom and top of the grooves). Thus neither the equations nor the field components of the staircase approximation tend toward the equations, or the field components for a smooth (sinusoidal) profile, however finite the truncation  $N$  is.

One of the possibilities for improving the convergence of the staircase approximation when the number of slices is large, in order to optionally avoid the numerical integration, is to use the set of Eqs. (1)–(3) with the vector normal to the sinusoidal profile (or the other nonstaircase profile to which the staircase approximation is applied) instead of Eqs. (5) and (6). This will not be correct for a smaller number of slices, because the set of Eqs. (1)–(3) must be used only for the true profile, whereas Eqs. (5) and (6) are valid for the multilamellar profile. But computations have shown that when  $M \rightarrow \infty$ , Eqs. (1)–(3) are

better suited to describe the fact that  $E_x$  or  $E_y$  is, in general, not continuous on the surface of an arbitrary shaped grating.

To that end, Fig. 12 presents the convergence rates of the different sets of Equations (1)–(3), (5) and (6), and (7) and (8) for a 20-step staircase profile. The numerical procedure is the following: Along the vertical  $y$  coordinate inside each slice (step), the coefficients in the differential set of equations to be integrated are taken constant (to permit use of the RCW method); however, these coefficients are calculated in three different manners [Eqs. (1)–(3), (5) and (6), and (7) and (8)]. As can be observed [Fig. 12(a)], the results are not satisfactory: While Eqs. (5) and (6) converge slowly but monotonically, Eqs. (7) and (8) converge more slowly; applying Eqs. (1)–(3) to the staircase profile gives better results for smaller  $N$ , but the improvement is not preserved for larger  $N$ . This shows that the number of slices  $M = 20$  is not sufficient to represent the “smooth” profile with the “smooth” set of Eqs. (1)–(3). However, if the wavelength is again increased to  $13 \mu\text{m}$  [Fig. 12(b)], as is already done in Fig. 11, the convergence rate of Eqs. (1)–(3) is quite rapid and the results are more stable (but still less stable than those obtained with the differential method). Note the zoom of the ordinate to reveal the differences between the different methods. The same conclusion is valid when the number of slices is increased to 200 slices with  $\lambda = 0.6328 \mu\text{m}$ ; the results obtained with Eqs. (1)–(3) and  $M = 200$  nearly coincide with the results of the differential method [always Eqs. (1)–(3)] applied to the sinusoidal profile [curve “diff.” in Fig. 4(a)]. Moreover, as already observed in Fig. 8, in that case the field is homogenized and no sharp peaks occur.

The conclusion is that if one is interested in the study of a true staircase profile having a comparatively low number of slices, so that the slice height is comparable with the wavelength, it is correct to use Eqs. (5) and (6), because they correctly describe the field discontinuities and the edge effects (sharp field peaks close to the ridges). When the methods are applied to the staircase approximation of a smooth arbitrary profile with a very large number of slices (theoretically, in the limit when  $M \rightarrow \infty$ ), it is much better to use the set of Eqs. (1)–(3), which better describe the effect of homogenization. However, this approach is equivalent to using the differential method (improved by the FFF technique) with the worse algorithm of integrating the differential equations: the rectangular rule. And indeed, when the number of slices is large and the coefficients of the system to be integrated are taken to be constant within each slice, whatever the method of integration may be, this is equivalent to integrating the system by using the rectangular rule with equidistant and fixed points of integration. It is well known that standard integration algorithms (e.g., Runge–Kutta or Adams–Moulton techniques) do much better.

Our conclusion, that when the slice height tends toward zero it is better to use Eqs. (1)–(3) than Eqs. (5) and (6), explains the observation made by Lalanne.<sup>22</sup> He considered a lamellar ( $M = 1$ ) grating in the low-modulation limit ( $h/d \rightarrow 0$ ). He found that the classical Eqs. (7) and (8) worked better than Eqs. (5) and (6), contrary to what

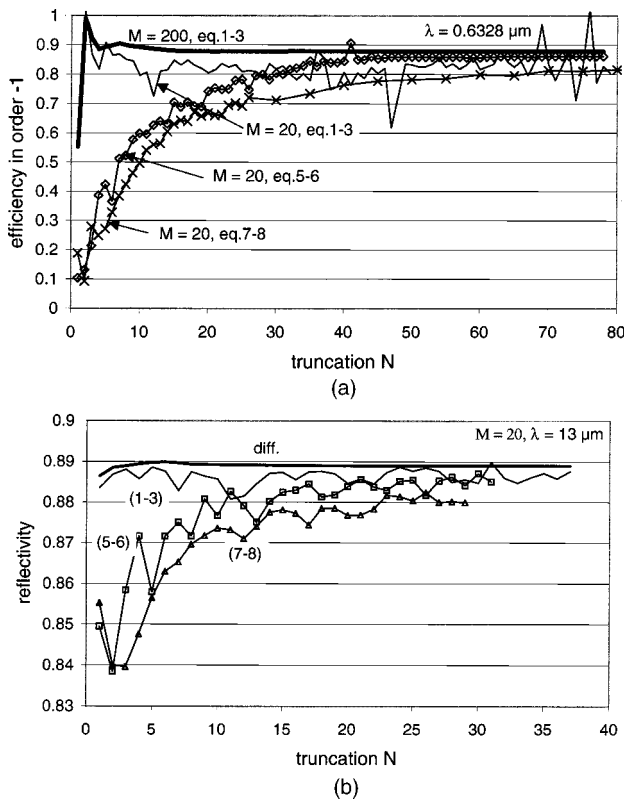


Fig. 12. Convergence rates of the RCW method compared when using the three different sets of equations as marked on the figure [Eqs. (1)–(3), (5) and (6), and (7) and (8)], compared with the differential method used for the sinusoidal profile. (a)  $\lambda = 0.6328 \mu\text{m}$ ,  $M = 20$ , and  $M = 200$ ; (b)  $\lambda = 13 \mu\text{m}$  and  $M = 20$ . The convergence of the differential method for a sinusoidal profile is shown by a solid curve marked “diff.”

happened for a finite-depth lamellar grating, for which Eqs. (7) and (8) failed to converge rapidly. As concluded here, when the slice height (equal to  $h/d$  for a single-step profile) tends toward zero, it is better to use Eqs. (1)–(3). However, in the case of a single-step lamella with  $h/d \rightarrow 0$ , Eqs. (1)–(3) tend toward Eqs. (7) and (8), because  $N_x \rightarrow 0$  and  $N_y \rightarrow 1$  everywhere along the profile. Thus it is better to use Eqs. (7) and (8) instead of Eqs. (5) and (6) when  $h/d \rightarrow 0$ . To repeat, the three approaches would become equivalent only without truncation.

## 7. CONCLUSION

The validity of the staircase approximation used to describe arbitrary-shaped gratings in the RCW and the modal methods is studied numerically. Although the approximation leads to reliable results in TE polarization, we show that for metallic gratings used in TM polarization, the profile ridges introduced by the staircase approximation cause sharp maxima in the local field. These maxima are independent of the method of modeling and are due to the replacement of the smooth profile by a staircaselike one. The maxima do not exist for the smooth profile. The number of maxima increase with the number of steps, which requires a greater number of basis functions (Fourier components or modes) to represent the field. No homogenization is observed when the number of the slices and/or the wavelength are increased, even when the number of steps exceeds 500 (with the step dimensions as small as wavelength/1300). This results from the choice of the way in which Maxwell equations are projected onto a truncated Fourier basis. When the correct projection is used by applying the rules for Fourier factorization of the products of discontinuous functions, as is done with the differential method, the convergence is much more rapid.

The conclusion is that although the RCW and the modal method are well suited for lamellar profiles or for gratings consisting of a stack of rectangular rods, because they lead to a short computation time they cannot compete with the differential method in the study of arbitrary-shaped metallic gratings in TM polarization.

## REFERENCES

1. M. G. Moharam and T. K. Gaylord, "Rigorous coupled-wave analysis of planar-grating diffraction," *J. Opt. Soc. Am.* **71**, 811–818 (1981).
2. M. G. Moharam and T. K. Gaylord, "Rigorous coupled-wave analysis of dielectric surface-relief gratings," *J. Opt. Soc. Am.* **72**, 1385–1392 (1982).
3. D. M. Pai and K. A. Awada, "Analysis of dielectric gratings of arbitrary profiles and thicknesses," *J. Opt. Soc. Am. A* **8**, 755–762 (1991).
4. M. Nevière and F. Montiel, "Deep gratings: a combination of the differential theory and the multiple reflection series," *Opt. Commun.* **108**, 1–7 (1994).
5. D. J. Zvijac and J. C. Light, "R-matrix theory for collinear chemical reactions," *Chem. Phys.* **12**, 237–251 (1976).
6. J. C. Light and R. B. Walker, "An R-matrix approach to the solution of coupled equations for atom-molecular reactive scattering," *J. Chem. Phys.* **65**, 4272–4282 (1976).
7. L. Li, "Formulation and comparison of two recursive matrix algorithms for modeling layered diffraction gratings," *J. Opt. Soc. Am. A* **13**, 1024–1035 (1996).
8. F. Montiel, M. Nevière, and P. Peyrot, "Waveguide confinement of Cerenkov second-harmonic generation through a graded-index grating coupler: electromagnetic optimization," *J. Mod. Opt.* **45**, 2169–2186 (1998).
9. P. Lalanne and G. Morris, "Highly improved convergence of the coupled-wave method for TM polarization," *J. Opt. Soc. Am. A* **13**, 779–783 (1996).
10. L. Li, "Use of Fourier series in the analysis of discontinuous periodic structures," *J. Opt. Soc. Am. A* **13**, 1870–1876 (1996).
11. E. Popov and M. Nevière, "Differential theory for diffraction gratings: a new formulation for TM polarization with rapid convergence," *Opt. Lett.* **25**, 598–600 (2000).
12. E. Popov and M. Nevière, "Grating theory: New equations in Fourier space leading to fast converging results for TM polarization," *J. Opt. Soc. Am. A* **17**, 1773–1784 (2000).
13. J. M. Elson and P. Tran, "Dispersion in photonic media and diffraction from gratings: a different modal expansion for the R-matrix propagation technique," *J. Opt. Soc. Am. A* **12**, 1765–1771 (1995).
14. G. Tayeb, "Dispersion in photonic media and diffraction from gratings: a different modal expansion for the R-matrix propagation technique: comment," *J. Opt. Soc. Am. A* **13**, 1766–1767 (1996).
15. L. C. Botten, M. S. Craig, R. C. McPhedran, J. L. Adams, and J. R. Andrewartha, "The dielectric lamellar diffraction grating," *Opt. Acta* **28**, 413–428 (1981).
16. G. Tayeb and R. Petit, "On the numerical study of deep conducting lamellar diffraction gratings," *Opt. Acta* **31**, 1361–1365 (1984).
17. S. E. Sandström, G. Tayeb, and R. Petit, "Lossy multistep lamellar gratings in conical diffraction mountings: An exact eigenfunction solution," *J. Electromagn. Waves Appl.* **7**, 631–649 (1993).
18. R. H. Morf, "Exponentially convergent and numerically efficient solution of Maxwell's equations for lamellar gratings," *J. Opt. Soc. Am. A* **12**, 1043–1056 (1995).
19. D. Maystre, "Integral methods," in *Electromagnetic Theory of Gratings*, R. Petit, ed., (Springer-Verlag, Berlin, 1980), Chap. 3.
20. G. Tayeb, "The method of fictitious sources applied to diffraction gratings," special issue on "Generalized Multipole Techniques (GMT)" of *Appl. Comput. Electromagn. Soc. J.* **9**, 90–100 (1994).
21. E. Popov and M. Nevière, "Maxwell equations in Fourier space: fast converging formulation for diffraction by arbitrary shaped, periodic, anisotropic media," *J. Opt. Soc. Am. A* **18**, 2886–2894 (2001).
22. P. Lalanne, "Convergence performance of the coupled-wave and the differential method for thin gratings," *J. Opt. Soc. Am. A* **14**, 1583–1591 (1997).